Design of an Optical Fiber Amplifier with Multiple Serial Pumping for Space Communications

Dirk Giggenbach

German Aerospace Research Establishment (DLR), Oberpfaffenhofen
Institute for Communications Technology
D-82230 Wessling, Germany

Proceedings of SPIE, Vol. 3110-2, p. 392

Presented at "The 10th Meeting on Optical Engineering in Israel", Jerusalem, 2 – 6 March 1997

ABSTRACT

The feasibility of an optical fiber amplifier as a booster amplifier for transmitter-terminals of free-space coherent laser communication systems has been investigated. To enhance the amplifier's efficiency and reliability in a harsh space environment a new pumping-scheme has been analyzed and demonstrated in an experimental set-up. The amplifier features efficient multiple serial coupling of the pump light into the multimode core of the double-clad fiber by using directional Y-couplers. Special attention has been paid to fiber-geometry, pump light absorption efficiency in the neodymium-doped single-mode core and the attenuation of pump and signal light.

Keywords: fiber amplifier, double-clad fiber, optical space communications, multimode Y-coupler

1. INTRODUCTION

The German Aerospace Research Establishment investigates the feasibility of coherent optical free space data transmission for links in satellite networks, between space probes, satellites and ground stations [1].
Nd-YAG lasers operating at 1064nm are used because of their good overall power efficiency combined with frequency stability, which is necessary for data transmission using phase modulation and coherent heterodyning in the receiver.
Though Nd-YAG lasers with the required output power (>1W) are now available, post-amplification in the transmitter is necessary because the integrated optical phase modulators cannot endure the high power levels. The modulators also cause around 5dB signal attenuation [2].
Double-clad fibers (DCF) with a Nd-doped inner signal core surrounded by a multimode pump light core are already used as single mode fiber lasers. DCFs can provide a sufficient single-pass gain when pump light intensity is optimized.
In this paper a means for cascaded multiple pump light leading based on directional multimode Y-couplers is introduced, theoretically examined and compared to experimental results. The proposed amplifier setup provides a modular design that enables redundant pump light sources and scaleable output power, both crucial in optical satellite communications.

2. EXPERIMENTAL SETUP

2.1 Structure and properties of the DCF

Using double-clad fibers for weakly pumped 4-level-system fiber amplifiers enables high-power multimode laser diodes as pump-sources, which can easily be launched into the large outer DCF multimode cladding. The used DCF (produced by IPHT, Jena) has a 5µm diameter single-mode signal core situated concentrically inside the 110µm diameter multimode pump light core. The outer cladding consists of silicon providing the required low refraction index. The pump light occasionally crosses the inner core and thereby excites the Nd-ions.

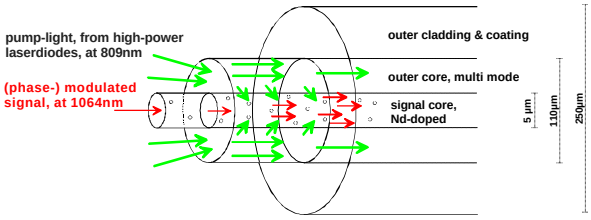

Fig.1 Cross section of the applied double-clad fiber

2.2 Pump light leading by Y-couplers

In a conventional DCF setup the pump light is end-coupled into the multimode core (MMC). This limits the number of pump sources to one laser diode (LD) at each end. By superpositioning two beams through polarizing beam splitter cubes, four LDs can be applied. The LDs are broad area emitters with $P_{PD,optical}$=1W at $\lambda_{0,p}$=809nm which matches well with the absorption bandwidth of the DCF at 804nm ±12nm. For the Y-coupler, the LD-power is first coupled into a multimode coupling fiber (CF) which guides the light into the DCF using a grinded directional multimode Y-coupler.

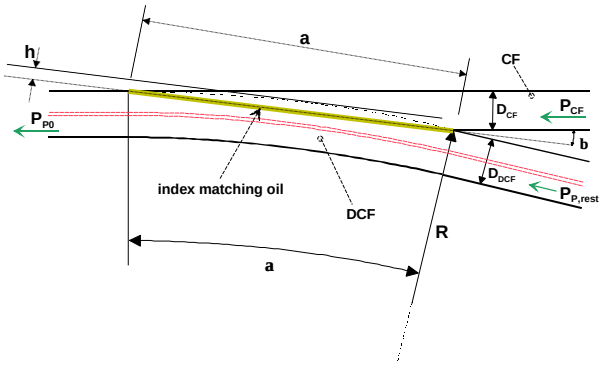

Fig.2 Cut through the multimode Y-coupler

For proper matching, the diameters of both surfaces should be equal. One can solve for the grind-depth "h" and DCF bend-radius "R":

$$h = \frac{D_{DCF-MMC}}{2} - \frac{\sqrt{D_{DCF-MMC}^{\ 2} - D_{CF}^{\ 2}}}{2} \qquad (1)$$

$$R = \frac{D_{CF}^{\ 2}}{8 \cdot h \cdot \sin^2(b)} + \frac{h}{2} \qquad (2)$$

The inner core of the DCF is not damaged by this process when $D_{DCF} > D_{CF}$. Using this geometry the axes of both fibers nearly merge into one another.

Index matching oil is needed, otherwise the unavoidable air gap between the two surfaces would cause total inner reflection of the pump light at the lapped fiber end of the CF. Bringing both areas close enough together (<1µm) allows for frustrated total inner reflection, however this was not feasible with standard grinding and positioning equipment. After the alignment process the two parts of the Y-coupler are fixed together and the index matching oil is sealed.

There are two main sources for loss of pump light at the Y-coupler. The small angle of incidence causes reflections at the transitions between the fibers and the index matching oil. To prevent total inner reflection, the relationship $n_{CF} < n_{oil} < n_{DCF-MMC}$ must be observed. At present there is no multimode fiber with exactly the DCF-MMC's refraction index commercially available.
The finite angle between CF and DCF causes an optical funnel and leads to radiation losses when steep rays exceed the DCF's maximum angle as shown in fig.3. This can be avoided by using a CF with a smaller numerical aperture (NA) than the DCF-MMC, but this lowers the LD-to-CF coupling efficiency.

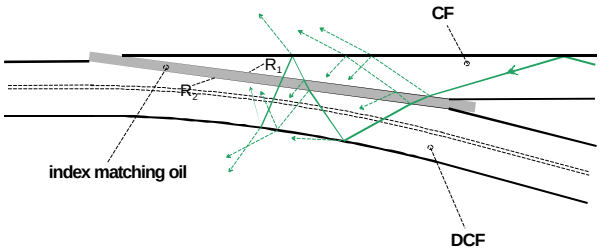

Fig.3 Radiation losses at the Y-coupler

The calculated achievable coupler efficiency is above 80%. Tests with different fibers and index matching oil combinations produced a coupling efficiency η_Y between 64% and 86%. With $P_{PD,optical}$ = 1W, the Y-coupler loss combined with the coupling loss between LD and CF (≈20%) allow for about 0.7W pump power to be introduced into the DCF-MMC.

The attenuation of pump light already inside the DCF before the coupler ("through-coupling attenuation") is approximately 70%.

A way to side-pump the DCF by micro-prisms has been reported by [7] and [12] but with lower coupling efficiency.

3. SIGNAL AMPLIFICATION MECHANISM

3.1 Rate equation of the simplified Nd-glass system

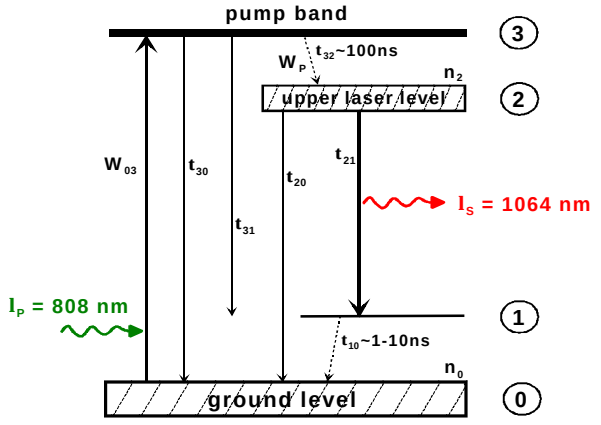

Fig.4 Simplified four level Nd-glass system

With τ_{32} and τ_{10} being very small compared to τ_{21} the rate equation becomes

$$\frac{dn_2(t,z)}{dt} = -s_{21}\cdot c\cdot f_{sig}(t,z)\cdot n_2(t,z) - \\ -\frac{1}{t_F}\cdot n_2(t,z) + h_p\cdot W_{03}(z)\cdot\left[n_{tot} - n_2(t,z)\right] \stackrel{!}{=} 0 \quad (3)$$

The change-rate of level-2 population equals the rate of pumped Nd-ions minus the rate of spontaneous and stimulated emission. In continuous-wave (cw) amplification this rate must be zero.
It will be shown that n_2 is always small against n_{tot} in the fiber amplifier so that the pump parameter W_{03} is not a function of n_2. The gaussian radial distribution of signal intensity inside the SMC has been approximated by a rectangular distribution so intensity ratios can be substituted with power ratios.

3.2 Absorption and attenuation of pump light

The effective absorption coefficient for 808nm inside the doped SMC is difficult to calculate due to the uncertain absorption cross section σ_{03} but has been measured at $23m^{-1}$ (100dB/m).
The absorption of pump light inside the DCF-SMC depends on the ability of MMC-rays to transit through the SMC. Ideally the pump light power inside the SMC ($P_{p,SMC}$) is given by the cross section ratio $\varepsilon_{p,SMC}$

$$P_{P,SMC} = e_{p,SMC}\cdot P_{P,MMC} \quad (4)$$

$$e_{p,SMC} = \frac{A_{SMC}}{A_{MMC}} \quad (5)$$

However the mode-selective absorption and reflections distort this simplified image.
The refraction index step between DCF-MMC and -SMC causes small power reflections away from the SMC for steeper angles of incidence, but reaches high values for flat angles of incidence (R=0,25 for φ=2° and R=0,5 for φ=1° in our DCF).
As [6] has shown, the absorption coefficient for pump light in a regularly coiled DCF over fiber length starts at a rate approximately twice that of $\varepsilon_{p,SMC}$, and after the absorption of the higher order axial modes drops to a value about ½ $\varepsilon_{p,SMC}$. Helical modes cannot be absorbed by the SMC. Mode mixing from helical to axial modes can be enhanced by periodically bending the winding of the DCF and by an excentric placement of the SMC or an asymmetric MMC cross section [5]. As the DCF in our experiment is wound up to enhance mode mixing, the cross section ratio is a sufficient approximation and will be applied to further calculations.

The low transparency of the silicon cladding causes an attenuation coefficient of $\alpha_{MMC}=0.007m^{-1}$ (30dB/km) for the total inner reflections at the MMC-silicon transition. The combined absorption and attenuation coefficient for the pump power is

$$a_{p,tot} = a_{MMC} + e_{p,SMC}\cdot a_{abs} \quad (6)$$

3.3 Amplification and attenuation of signal light

At $P_{sig} = P_{sat}$ spontaneous emission equals stimulated emission. P_{sat} has been calculated through the measured fluorescence lifetime τ_f = 360µs to be 6mW. The inversion-ratio for $P_{sig} << P_{sat}$ (small signal inversion) can be calculated according to

$$\frac{n_{2,small}}{n_{tot}} = \frac{W_P\cdot t_f}{W_P\cdot t_f + 1} \quad (7)$$

For our amplifier, this ratio could theoretically reach 26% at coupler locations with 2W pump light absorbed optimally and no stimulated emission present. With $P_{sig} >> P_{sat}$ (amplifier operating at saturation) this ratio falls to approx. 4% and thus bleaching of the ground state will not occur. This fact helps us to calculate the pump rate $W_p(z)$.

$$W_p(z) = h_p\cdot W_{03}(z) \quad (8)$$

$$h_p = \left(1 + \frac{t_{32}}{t_{31}} + \frac{t_{32}}{t_{30}}\right)^{-1} \le 1 \quad (9)$$

$$W_{03}(z) = s_{03}\cdot c\cdot f_P(z) \quad (10)$$

$$f_p(z) = e_{p,SMC}\cdot\frac{P_{p,MMC}(z)}{A_{SMC}(h\cdot c\cdot n_{808})} \quad (11)$$

The branching ratio η_p represents losses by pumped Nd-ions that do not end up at the upper laser level. For our fiber $\eta_p \approx 0.9$. The small-signal gain ($P_{sig} << P_{sat}$) is then

$$g_0(z) = s_{21}\cdot n_{tot}\cdot\frac{W_p(z)\cdot t_f}{W_p(z)\cdot t_f + 1} = s_{21}\cdot n_2 \quad (12)$$

and the effective gain with applied signal power

$$g(z) = \frac{g_0(z)}{1 + \frac{P_{sig}(z)}{P_{sat}}} \qquad (13)$$

The absorption coefficient α_{sig} caused by the necessary silica dopents is much smaller than in laser crystals, but it becomes a significant design parameter due to the long signal path through the DCF.
The signal power builds up along z according to

$$\frac{dP_{sig}(z)}{dz} = g(z) \cdot P_{sig}(z) - a_{sig} \cdot P_{sig}(z) \qquad (14)$$

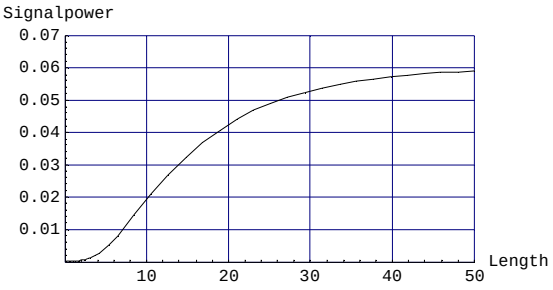

Fig.5 Typical numerical solution of (14) with $P_p(z)$=const. and an initial signal power $P_{sig0} << P_{sat}$.

Three different gain regions can be distinguished in Fig.5. First P_{sig} rises exponentially with g(z) ≈ constant. When $P_{sig} > P_{sat}$, g(z) starts to fall which causes a net linear growth of P_{sig}. Finally, the gain equals the attenuation and amplification no longer occurs. In an optimized amplifier setup one can avoid the inefficient first meters before $P_{sig} >> P_{sat}$ by starting with a signal power above saturation (e.g. with 30mW). This is also important from a communication-technological point of view, because a low P_{sig0} allows a high amount of amplified spontaneous emission (ASE).

Fig.5 is not a realistic representation because P_p is not constant over z and therefore $W_p(z)$ and g(z) vary as described in the following sections.

4. GAIN WITH DIFFERENT PUMPING SCHEMES

In a fiber amplifier the development of W_{03} and thus g depend on the way the pump power is coupled to the fiber. By varying the location and orientation of the Y-couplers, total signal gain and power efficiency can be influenced.

4.1 Pumping schemes for one DCF section

4.1.1 Co-directional pumping

The pump light power over fiber length for pumping in the signal direction at z=0 with $P_{p0,c,MMC}$ is

$$P_{p,c,MMC}(z) = P_{p0,c,MMC} \cdot \exp\left(-a_{p,tot} \cdot z\right) \qquad (15)$$

with $\alpha_{p,tot}$=0.0645m^{-1} for our DCF. Numerical solutions are shown in fig.6 for three different initial signal powers and two different pump powers.

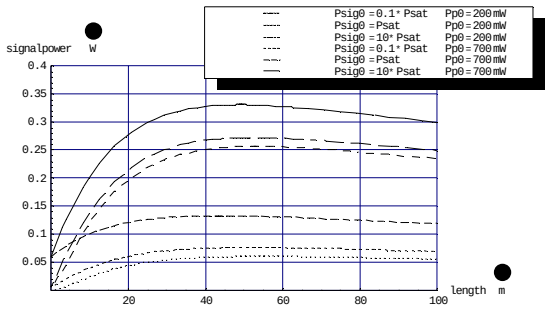

Fig.6 Co-directional pumping with small P_{sig0}

In contrast to Fig.5 the signal degenerates when the pump intensity diminishes. With higher initial signal powers the maximum output power is reached after a shorter fiber section.

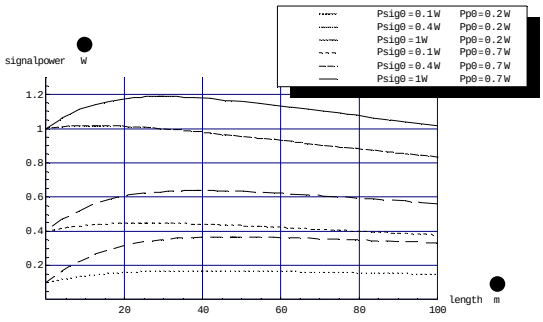

Fig.7 Co-directional pumping with large P_{sig0}

The gain is decreasing and higher pump power is required to overcome attenuation and obtain useful amplifications.

4.1.2 Reverse pumping

In the case of reverse pumping at z=L in the negative z-direction, we derive

$$P_{p,r,MMC}(z) = P_{p0,r,MMC} \cdot \exp\left(-a_{p,tot} \cdot (L-z)\right) \qquad (16)$$

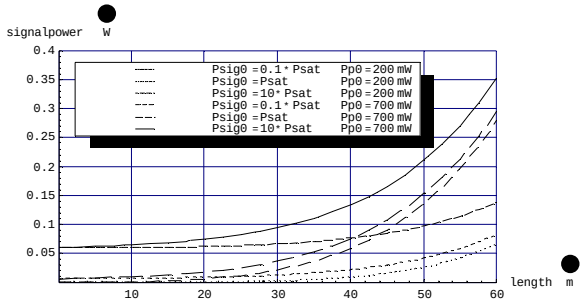

Fig.8 Numerical solutions for reverse pumping at L=60m with same P_{p0} and P_{sig0} as in fig.6

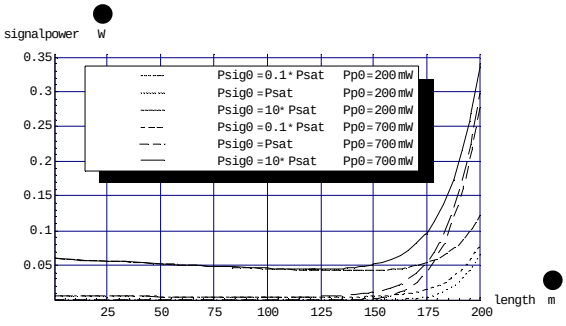

Fig.9 Numerical solutions for reverse pumping with same P_{p0} and P_{sig0} as in fig.6 for L=200m

No signal reduction takes place at the end of the section because pump power grows steadily with signal power towards the coupler. But too long a section leads to attenuation at the beginning. However this does not affect signal output very much for small P_{sig0}. The effective gain is slightly higher than in the co-directional pumping case.

With higher initial signal powers, the attenuation due to excessive fiber length rises significantly and the optimum fiber length is shorter.

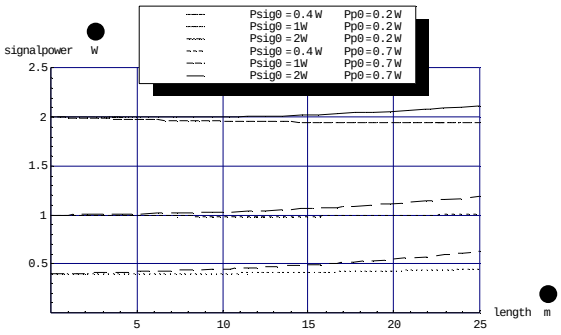

Fig.10 Numerical solutions for reverse pumping with high P_{sig0} and optimum L

4.1.3 Bi-directional pumping

Pumping from both section ends with $P_{p0,c}$ at z=0 and $P_{p0,r}$ at z=L results in the following pump power distribution

$$P_{p,b,MMC}(z) = P_{p0,c,MMC} \cdot \exp\left(-a_{p,tot} \cdot z\right) + \\ + P_{p0,r,MMC} \cdot \exp\left(-a_{p,tot} \cdot (L-z)\right) \qquad (17)$$

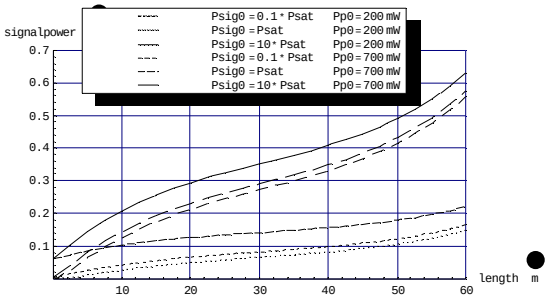

Fig.11 Bi-directional pumping with small P_{sig0} and optimum L

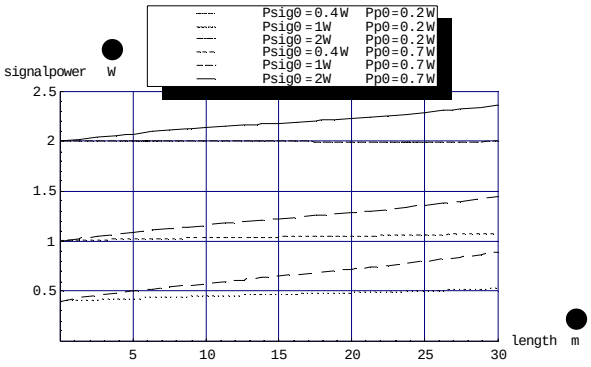

Fig.12 Bi-directional pumping with large P_{sig0} and optimum L

4.1.4 Discussion of the three cases

Higher pump power causes a better average gain coefficient with high P_{sig0} and therefore efficiency rises with stronger LDs.
The optimum fiber length gets shorter as P_{sig0} increases.
Combinations of co- and reverse-pumping must take into account the optimum fiber length which is derived by the preceding calculations.
In all three cases fiber length is relativly uncritical when P_{sig} is small and becomes crucial with higher powers because of the attenuation inside the SMC.

4.2 Cascaded multiple pumping

This section discusses signal amplification for one of the several possible pumping schemes.

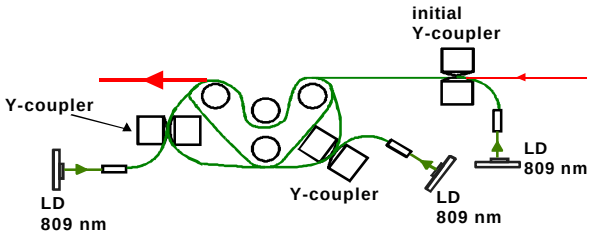

Fig.13 Example for a multiple pumped amplifier constellation. The kidney-shaped winding enhances mode-scrambling.

The investigated setup has an initial reverse-pumping coupler followed by seven bi-directional pumped fiber sections. P_{sig0} = 5*P_{sat} and P_{p0}=700mW at every Y-coupler has been presumed.

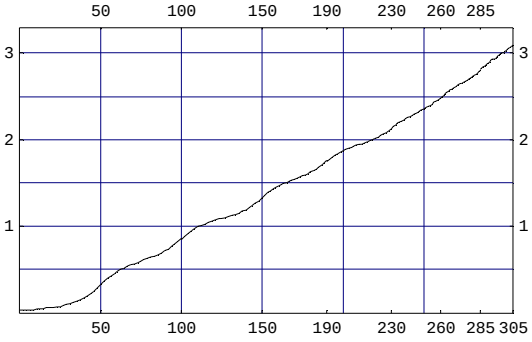

Fig.14 Growing of P_{sig} with cascaded bi-directional pumping and optimized fiber section lengths. Couplers are positioned at the marked lengths.

The signal output power after 305m of DCF is 3.1W. This means an efficiency of 3.1W / (0.7 * 15W) = 0.30 inside the DCF.
The remaining pump power from the preceding fiber section is hereby supposed to be totally attenuated inside the Y-Coupler. Through-coupling of this power can be enhanced by optimizing the coupler geometry with this aspect. An arrangement as depicted in Fig.15 would provide the highest gain and efficiency for one fiber section. Methods to enhance through-coupling are discussed in section 6.

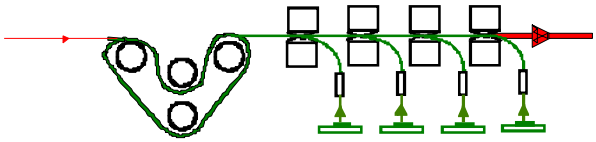

Fig.15 Summing up the powers of several LDs with improved Y-couplers.

5. RESULTS

Directional multimode Y-couplers have been practically tested to couple up to 86% of pump light from a standard multimode fiber into a DCF-MMC.
The feasibility of building a cascaded multiple pumped DCF amplifier with output greater than 3W has been shown by simulation.
The total calculated system efficiency (socket-to-$P_{sig,out}$)

$$h_{tot} = h_{LD,el\rightarrow opt} \cdot h_{LD\rightarrow CF} \cdot h_Y \cdot h_{abs,SMC} \cdot h_{808\rightarrow 1064} \cdot h_p \cdot h_{gain}$$

lies between 7% and 14%, depending on the applied constellation. The CF-to-output efficiency (without $\eta_{LD,el\text{-}opt}$ and $\eta_{LD\text{-}CF}$) is then between 20% and 40%.
With higher required output powers the fiber sections between the couplers must be shortened to maintain a high pump rate. This leads to a lower $\eta_{abs,SMC}$ because remaining pump light inside the DCF is radiated out of

the Y-coupler. At P_{sig} > 12W the applicable pump power becomes too weak to maintain a positive gain even with bi-directional pumping and very short sections.

6. CONCLUSION AND IMPROVEMENTS

Losses of remaining pump light at the Y-couplers ("through-coupling-efficiency") can be reduced be using a smaller CF as this loss is proportional with the size of the coupler's transitional area. Ignoring the problem of poorer laser diode to CF coupling allows narrower positioning of the couplers and thus enhances W_p without losing the pump light from the preceding coupler. Much higher signal output power could then be achieved. This variant has not yet been investigated because our couplers attenuate the remaining pump light too much. However high power laser diodes with improved beam quality are now commercially available, so efficient coupling from the LDs into a pigtailed CF of about 50µm is now feasible.

A computer ray-tracing model of the Y-coupler is being set up to find the optimum coupler geometry. This model will also take into account multiple back-reflections along the coupler length, losses by rays that exceed the fibers' N.A., helical modes, polarization dependent effects and losses by non-optimum surface-shapes and alignment. It would also allow investigations of the mode-distribution and the helical-ray ratio inside the DCF-MMC.

The silicon cladding causes problems due to the attenuation of the pump light and its susceptibility to damage. Its thermal instability prevents the construction of a fused Y-coupler between the pump fiber and the DCF. The fiber producer is currently working on a hard-cladding to replace the silicon. A fused coupler combined with matching refraction indices of pump fiber and DCF-MMC would have the lowest coupling losses.
Besides, the DCF can not be glued tightly enough to the polishing block with the soft silicon and so the glass core sometimes breaks during the polishing process, another argument for a hard outer cladding.

Higher Nd-doping will increase the small signal gain coefficient. However from a certain concentration on the Nd-ions tend to build clusters and thus the signal attenuation rises stronger than the overall gain improves. Optimum has to be found.
A smaller MMC to SMC cross-section ratio (maximum possible single mode diameter is approx. 7.5µm) also increases the pump rate inside the SMC.
Increasing of τ_f could reduce losses by spontaneous emission and thus increase amplifier gain and overall efficiency. The ASE would become smaller and thus the additional signal noise would diminish. In certain Nd-glass, a τ_f of 600µs has been observed.

Rayleigh-Scattering has not been regarded as an additional noise source, because after the amplifier fiber there is free space transmission and thus no further scattering takes place like in fiber communications.

Only one variation of several possible coupler constellations could be investigated in this paper as an optimum design depends on too many parameters. A tradeoff must be found between output power and other amplifier requirements, i.e. overall power efficiency, redundancy for LD failures and scaleability of output power.

The concept of multiple cascaded pumping by Y-couplers offers a wide variety of DCF-amplifier setups to fulfill the application-specific differing demands.

7. ACKNOWLEDGMENTS

The author wants to thank Prof. Manfred Fickenscher (FH Munich) for helpful discussions and his preceding work on the DCF amplifier and Anton Schex (DLR) for his help with the mathematics.

8. REFERENCES

[1] C. Rapp, B. Wandernoth, G. Steudel, A. Schex, DLR Experimental Systems for Free Space Optical Communications, Optical Communications Technology Laser '93, Munich, Germany, June 1993

[2] M. Fickenscher, R. Heilmann, Optische Komponenten für die Weltraumkommuniukation, Z. Flugwiss. Weltraumforsch. 20 (1996) P.18-30, Springer-Verlag 1996

[3] W. Koechner, Solid-State Laser Engineering, Vol. 1, Springer Series in Optical Sciences, 4th Ed., Springer, Berlin, 1996

[4] M. V. Klein, T.E. Furtak, Optik, Springer, Berlin, 1988

[5] A. Tünnermann, H. Zellmer, H. Welling, Faserlaser - Neuartige Laserstrahlquellen mit Emissionen im sichtbaren Spektralbereich, Physikalische Blätter 52 (1996), Nr. 11, p.1123

[6] S. Bedö, W. Lüthy, H. P. Weber, The effective absorption coefficient in double-clad fibers, Optics Communications 1993, p. 331

[7] W. Lüthy, H. P. Weber, High-power monomode fiber lasers, Optical Engineering, August 1995, Vol. 34 No. 8, p. 2361

[8] M. Fickenscher, Efficient Optical Amplifier for Use in Coherent Space Communication, Proceedings of the

12th International Congress Laser95 Munich 1995, 324-327

[9] Zellmer, et al., High-power cw neodymium-doped fiber laser operating at 9.2 W with high beam quality, Optics Letters 20 (1995) 578-580

[10] G. J. Ainslie, S. P. Craig, S. T. Davey, The Absorption and Fluorescence Spectra of Rare Earth Ions in Silica-Based Monomode Fibers, J. o. Lightwave Technology, Vol. 6, No. 2, Feb. 1988

[11] J. Stein, Untersuchungen an einem Neodym-Faserverstärker zur Satellitenkommunikation, diploma thesis, German Aerospace Research Establishment, 1997

[12] Th. Weber et al., A longitudinal and side-pumped single transverse mode double-clad fiber laser with a special silicone coating, Optics Communications 115 (1995) 99-104

9. SUMMARY OF DCF PROPERTIES

NA_{MMC}	0.38	1
NA_{SMC}	0.14	1
n_{Nd}	$3 * 10^{25}$ [1300ppm]	m^{-3}
τ_f	360	µs
P_{sat}	0.006	W
α_{MMC}	0.007 [30dB/km]	m^{-1}
α_{abs}	23 [100dB/m]	m^{-1}
α_{sig}	0.0028 [12dB/km]	m^{-1}
σ_{03}	$\approx 1 * 10^{-24}$	m^2
σ_{21}	$\approx 1.1 * 10^{-24}$	m^2
c	$1.95 * 10^8$	m/s
ν_{1064}	$2.8 * 10^{14}$	s^{-1}
ν_{808}	$3.7 * 10^{14}$	s^{-1}
η_p	≈ 0.9	1

10. ABBREVIATIONS

DCF	double-clad fiber
SMC	single mode core
MMC	multi mode core
LD	laser diode
CF	coupling fiber, carrying the pump light from the laser diode into the DCF
W_p	pump rate
W_{03}	pump parameter
ϕ_p	photon-flux of pump light inside DCF-SMC
ϕ_{sig}	photon-flux of signal light inside DCF-SMC
η_p	pumping efficiency ("branching ratio")
$\varepsilon_{p,SMC}$	transit coefficient for pump light from MMC through SMC
α_{sig}	att. coeff. of signal light in the SMC
α_{MMC}	att. coeff. of pump light in the MMC
α_{abs}	absorption coeff. of pump light in the SMC
α_{tot}	combined absorption and attenuation coeff. of pump light
σ_{03}	absorption cross section of Nd for 809nm
σ_{21}	stimulated emission cross section of Nd for 1064nm
τ_F	fluorescence lifetime without stimulated emission
c	speed of light inside the DCF
P_{sat}	saturation signal power
P_{p0}	inserted multimode pump power at Y-coupler
P_{sig0}	signal power at the start of one fiber section
g_0	small signal gain coefficient
g	actual signal gain coefficient
ASE	amplified spontaneous emission